

Cy3 one from the same gel so that gel-to-gel differences were compensated, using the DeCyder images software (GE Healthcare Biosciences). System reproducibility was verified by comparing the protein profiles obtained from three independent separations of the identical sample (sample 1, Table 1 and Supplemental Table 1). Scatter plot analysis revealed that the standardized intensity of more than 96% of the spots ranged within a 2-fold difference (Fig. 1B). Representative 2D images with the numbers of the identified spots are shown in Fig. 1A. An enlarged 2D image is shown in Supplemental Fig. 1.

2.3. Data analysis

Data analyses that included the hierarchical cluster analysis were performed using the Expressionist software (Genedata, Bersel, Switzerland).

2.4. Protein identification by mass spectrometry

Proteins corresponding to the spots of interest were identified by mass spectrometry according to our previous report [18–20,22,29,30]. Cy5-labeled proteins separated by 2D-PAGE were recovered in gel plugs and digested with modified trypsin (Promega, Madison, WI). The trypsin digests were subjected to liquid chromatography coupled with tandem mass spectrometry using a Finnigan LTQ linear ion trap mass spectrometer (Thermo Electron Co., San Jose, CA) equipped with a nano-electrospray ion source (AMR Inc., Tokyo, Japan). The Mascot software program (version 2.1, Matrix Science, London, UK) was used to search for the mass of the peptide ion peaks against the SWISS-PROT database (Homo sapiens, 12,867 sequences in Sprot_47.8 fasta file). A Mascot score of 35 or higher was considered to indicate positive protein identification. When multiple proteins were identified in a single spot, the proteins with the highest number of peptides were considered to be those corresponding to the spot.

2.5. Functional classification of the identified proteins

Functional classification of the identified proteins was based on their classification in Gene Ontology (<http://www.geneontology.org>) (Table 2 and Supplemental Table 2).

2.6. Production of rabbit polyclonal antibody

We synthesized peptides corresponding to the peptide sequences 354–370 of full-length secernin-1 and then immu-

nized rabbits. Antiserum was purified by affinity column chromatography using an antigen peptide coupled with solid-phase column. The specificity of the produced secernin-1 fragment was confirmed by Western blotting (Supplemental Fig. 2). The proteins corresponding to the western blotting signal were examined using mass spectrometry, and the peptides of secernin-1 were identified (Supplemental Table 3).

2.7. Western blotting and Immunohistochemical examination of secernin-1 expression

Protein samples were separated by SDS-PAGE and subsequently blotted on a nitrocellulose membrane. The membrane was incubated with rabbit polyclonal antibody against secernin-1 (1:200 dilution), and then horseradish peroxidase-conjugated secondary antibody (1:1000 dilution, GE Healthcare Biosciences). Signal was detected using an enhanced chemiluminescence system (GE Healthcare Biosciences) and LAS 3000 (Fuji film, Tokyo, Japan). For immunohistochemical studies, four micrometer-thick tissue sections were autoclaved in 10 mM citrate buffer (pH 6.0) at 121 °C for 30 min, and incubated with the antibody against secernin-1 (1:200 dilution). Immunostaining was performed using the biotin-free horseradish peroxidase enzyme-labelled polymer of the Envision Plus detection system (DAKO, Carpinteria, CA). Two certified pathologists (N.T. and D.K.) examined the stained sections in a blinded fashion regarding clinical. The few discrepancies noted between the two observers were resolved by re-examination of the sections.

2.8. Molecular analysis

We examined 31 of 45 cases for which RNA samples were available for the presence of the SYT-SSX1 and SYT-SSX2 fusion genes. Reverse transcription-polymerase chain reaction (RT-PCR) was done using the primers SYT 5'CAA CAG CAA GAT GCA TAC CA3', SSX1 5'GGT GCA GTT GTT TCC CAT CG3' and SSX2 5'GGC ACA GCT CTT TCC CAT CA3' followed by direct sequencing (Table 1 and Supplemental Table 1) [11,31].

2.9. Statistical analysis

The tumor specific- and metastasis free-survival times were calculated from the first treatment of the primary tumor to death from tumor specific causes or to first evidence of metastasis, respectively. All time-to-event endpoints were computed by the Kaplan–Meier method. Patients who died of

Fig. 1 – Identification of proteins differentially expressed in synovial sarcoma. (A) Representative 2D image of proteins detected in synovial sarcoma tissues. The protein spots in red are those highly expressed in the P-SS group, and the blue spots were highly expressed in the G-SS group. **(B)** Evaluation of the reproducibility of 2D-DIGE by scatter grams. Sample 1 (Table 1) was examined in triplicate gels independently. **(C)** Hierarchical clustering of the 13 synovial sarcoma cases based on the intensity of the 20 protein spots. The cases are color-coded as red (P-SS) or light green (G-SS) as indicated in the panel. The case numbers correspond to those in Table 1. The spot numbers and the protein names are shown on the right side and correspond to those in Table 2. In order to perform the hierarchical clustering analysis, these expression values in C underwent numerical corrections by the data mining software program (Expressionist software program, Genedata, Bersel, Switzerland), based on the values of the raw expression data that were acquired by 2D-DIGE. Finally, in this figure, these expression values were indicated by modified scores ranging from 0 to 1.0.

Table 2 – Differentially expressed proteins corresponding to the prognosis of synovial sarcomas (good prognosis cases vs poor prognosis cases).

Spot No ^a	Accession no ^b	Symbol	Identified protein ^b	Wilcoxon test p value	Fold difference	pI ^d	pI ^d (obs) ^c	MW (obs) (kD) ^c	MW (kD) ^d	Protein score ^e	Peptide matches	Sequence coverage (%)	Function ^d
260	P02787	TRFE	Serotransferrin precursor	8.081E-03	3.218	6.55	6.81	105.6	77.1	134	3	4.4	Ion transportation
267	Q14697	GANAB	Neutral alpha-glucosidase AB precursor	6.216E-03	1.861	5.89	5.74	105.6	106.8	287	5	6.6	Carbohydrate metabolic process
300	P14314	GLU2B	Glucosidase II beta subunit precursor	6.216E-03	1.955	4.46	4.34	102.4	59.3	190	3	6.5	Protein kinase cascade
315	P08238	HS90B	Heat shock protein HSP 90-beta	2.525E-03	2.157	5.00	4.97	102.4	83.1	82	2	3.0	ATP binding
451	P14625	ENPL	Endoplasmic precursor	9.524E-03	2.342	5.09	4.76	85.5	92.5	78	2	2.9	Anti-apoptosis
649	Q9UHD9	UBQL2	Ubiquilin-2	1.554E-03	2.157	5.07	5.24	74.3	65.8	88	2	4.2	Proteasome-mediated
856	P61158	ARP3	Actin-related protein 3	6.061E-03	1.831	5.57	5.61	57.5	47.3	372	7	20.6	Cell motion
903	P14625	ENPL	Endoplasmic precursor	6.216E-03	1.722	4.84	4.76	59.3	92.5	89	2	2.2	Anti-apoptosis
972	Q12765	SCRN1	Secernin-1	1.554E-03	2.246	4.63	4.66	51.9	46.4	100	2	4.3	Exocytosis
978	Q12765	SCRN1	Secernin-1	1.554E-03	2.564	4.64	4.66	51.9	46.4	100	3	4.8	Exocytosis
1027	Q12765	SCRN1	Secernin-1	2.525E-03	2.050	4.66	4.66	50.0	46.4	137	2	5.3	Exocytosis
1030	P06733	ENOA	Alpha enolase	1.554E-03	1.911	6.02	6.99	51.9	47.0	198	6	8.5	Transcription
1153	Q9NVA2	SEP11	Septin-11	1.554E-03	1.688	6.86	6.38	46.9	49.3	278	6	14.7	Cell cycle
1411	Q9UJ70	NAGK	N-acetylglucosamine kinase	6.216E-03	1.347	5.89	5.82	37.6	37.2	180	3	10.8	N-acetylglucosamine metabolic process
1634	P50402	EMD	Emerin	1.554E-03	2.262	5.36	5.29	32.7	29.0	254	4	16.9	Muscle contraction
1723	Q06323	PSME1	Proteasome activator complex subunit 1	8.081E-03	1.513	5.86	5.78	30.9	28.7	264	5	22.1	Ubiquitin-dependent
1725	P67936	TPM4	Tropomyosin alpha 4 chain	3.108E-03	1.657	4.61	4.67	30.6	28.4	835	20	34.4	Cell motion
1920	Q9NR31	SAR1A	GTP-binding protein SAR1a	1.554E-03	1.462	6.63	6.21	22.9	22.4	132	2	11.6	ER-Golgi transport
2004	P84085	ARF5	ADP-ribosylation factor 5	6.216E-03	1.590	6.30	6.36	21.9	20.4	221	4	21.2	Protein transport
2063	P60660	MYL6	Myosin light polypeptide 6	4.040E-03	3.863	4.38	4.56	19.6	16.9	193	4	35.8	Muscle filament sliding

^a Spot numbers refer to those in Fig. 1A and Supplemental Fig. 1.

^b Accession numbers of proteins were derived from Swiss-Prot and NCBI nonredundant databases.

^c Observed isoelectric point and molecular weight calculated according to location on the 2-D gel.

^d Theoretical isoelectric point and molecular weight obtained from Swiss-Prot and the ExPASy database. (<http://au.expasy.org>).

^e Mascot score for the identified proteins based on the peptide ions score ($p < 0.05$) (<http://www.matrixscience.com>).

causes unrelated to synovial sarcoma were censored at the time of death. Potential prognostic factors were identified by uni-variate analysis using the log-rank test. Independent prognostic factors were evaluated using a Cox's proportional hazards regression model and a stepwise selection procedure. To arrive at a parsimonious multivariate model, covariates were selected into the model only if they contributed significantly to the fit of the model based on the chi-square test value. *P* differences <0.05 were considered to be significant. Statistical analyses were performed using the SPSS statistical package (SPSS, Chicago, Illinois).

3. Results

We compared the protein expression profiles between eight G-SS and five P-SS cases using 2D-DIGE. We selected 1663 protein spots that appeared in at least 75% of the images of the Cy3-labeled internal control sample for further analysis, to decrease irrelevant expression data. As this selection was based on the observation of the gel images of common internal control sample, it did not eliminate spots that were absent/present between the G-SS and P-SS groups. The G-SS and P-SS samples were not classified into their respective groups based on the overall protein expression features consisted with the intensity of 1663 protein spots (data not shown). We found that 20 protein spots had significantly different intensity between the two groups ($p < 0.01$). The localization of the 20 spots on the 2D image is demonstrated in Fig. 1A (an enlarged image is shown in Supplemental Fig. 1). Hierarchical clustering analysis accurately classified the 13 synovial sarcoma samples into either the G-SS or the P-SS group based on the intensity of these 20 selected spots (Fig. 1C and Supplemental Fig. 3). Mass spectrometric protein identification revealed that the 20 protein spots corresponded to 17 distinct gene products (Fig. 1C, Table 2 and Supplemental Table 2).

Three of the 20 protein spots were identified as corresponding to secernin-1 and all three had higher intensity in the good prognosis patient group (Supplemental Fig. 4). Secernin-1 is highly expressed in gastric and colon cancer [25], but its association with synovial sarcoma has not been reported to date.

We therefore further examined the relationship of the expression of secernin-1 with the malignant potential of synovial sarcoma. Western blotting confirmed the relationship of secernin-1 expression with the outcome of synovial sarcoma using our original secernin-1 polyclonal antibody. The relative protein amounts measured by 2D-DIGE and Western blotting highly correlated with the prognosis groups for all protein spots (fold-difference: 4.969, $p < 0.0001$) (Fig. 2A and B). Immunohistochemistry showed that secernin-1 expression was higher in the good prognosis synovial sarcoma compared with the poor prognosis synovial sarcomas (fold-difference: 4.969, $p < 0.0001$) (Fig. 2C).

We further validated the relationship of secernin-1 expression with the malignant potential of synovial sarcoma in further 45 synovial sarcoma cases using immunohistochemistry. Being consistent with the previous reports [24–26] (<http://www.uniprot.org/uniprot/Q12765>), secernin-1 expression was observed mainly in the cytoplasm (Fig. 2C and Supplemental

Fig. 5). We decided that cases with cytoplasm staining for secernin-1 were considered as secernin-1 positive, whereas cases without staining for secernin-1 were considered as secernin-1 negative.

Among the 45 patients in this study, 15 patients were alive and continuously disease free, five patients were alive with no evidence of disease, four patients were alive with disease and 21 patients had died of the disease in the follow-up period (median 82.1 months; range 8 to 318 months) (Supplemental Table 1). Immunohistochemistry revealed that 13 of 18 patients who had died had a secernin-1 negative primary tumor and 18 of 27 patients who were alive had a secernin-1 positive primary tumor (χ^2 : $p = 0.0170$). Secernin-1 localized in nucleus in majority of cases, and we did not find the correlation between secernin-1 localization and clinico-pathological parameters (Supplemental Fig. 5 and Supplemental Table 4). The 5-year survival rate for patients with secernin-1 positive and negative tumors was 77.6% and 21.8% respectively ($p = 0.0015$; log-rank test, Fig. 3A and Table 3).

Distant metastasis was observed in a significantly higher proportion of patients with secernin-1 negative tumors compared with those with secernin-1 positive tumors (15/18 vs 12/27 cases, χ^2 : $p = 0.0140$), with a median follow-up period of 65 months. The 5-year metastasis free survival rate was significantly higher in the patients with the secernin-1 positive primary tumors than in those with negative ones (62.8% vs 16.7%; $p = 0.0012$; log rank test, Fig. 3B and Table 3).

Univariate analysis revealed that high grade (III) ($p = 0.0003$), stage IV ($p < 0.0001$), presence of metastatic disease at diagnosis ($p < 0.0001$) and negative secernin-1 staining ($p = 0.0015$) correlated significantly with poor prognosis for tumor specific survival (Table 3). There was no correlation between the expression of secernin-1 and other clinico-pathological parameters examined. No other factors were associated with tumor specific survival, including age, gender, site, fusion gene, size, depth, local recurrence, adjuvant chemotherapy, and adjuvant radiotherapy (Table 3). The poorly differentiated histological subtype ($p < 0.0001$), high MIB-1 index ($p = 0.0049$), high histological grade ($p < 0.0001$), and negative secernin-1 staining ($p = 0.0012$) correlated with low metastasis free survival rate.

The samples used ranged from 1970 to 2005 collection date, and the storage dates might affect the quality of protein samples. To clarify this issue, we compared the 13 samples obtained between 1979 and 2000 and the 32 samples between 2000 and 2005. We found that there was no statistically significant difference for the immunohistological expression between these groups. We also compared the prognosis between two groups, and found that there was no statistical significant difference between these two groups (5-years overall survival: $p = 0.5995$ and 5-years metastasis free survival: $p = 0.6626$).

A multivariate survival analysis revealed that both negative secernin-1 staining and the presence of metastatic disease at the time of diagnosis significantly correlated with low tumor specific survival rate, and were the two most prominent negative factors predictive of short tumor specific survival (Table 3). Large (>5 cm) tumor size ($p = 0.0220$), high MIB-1 index ($p = 0.0070$), high histological grade ($p = 0.0020$) and negative secernin-1 expression ($p = 0.0010$) were also independent factors for short a metastasis free survival (Table 3).

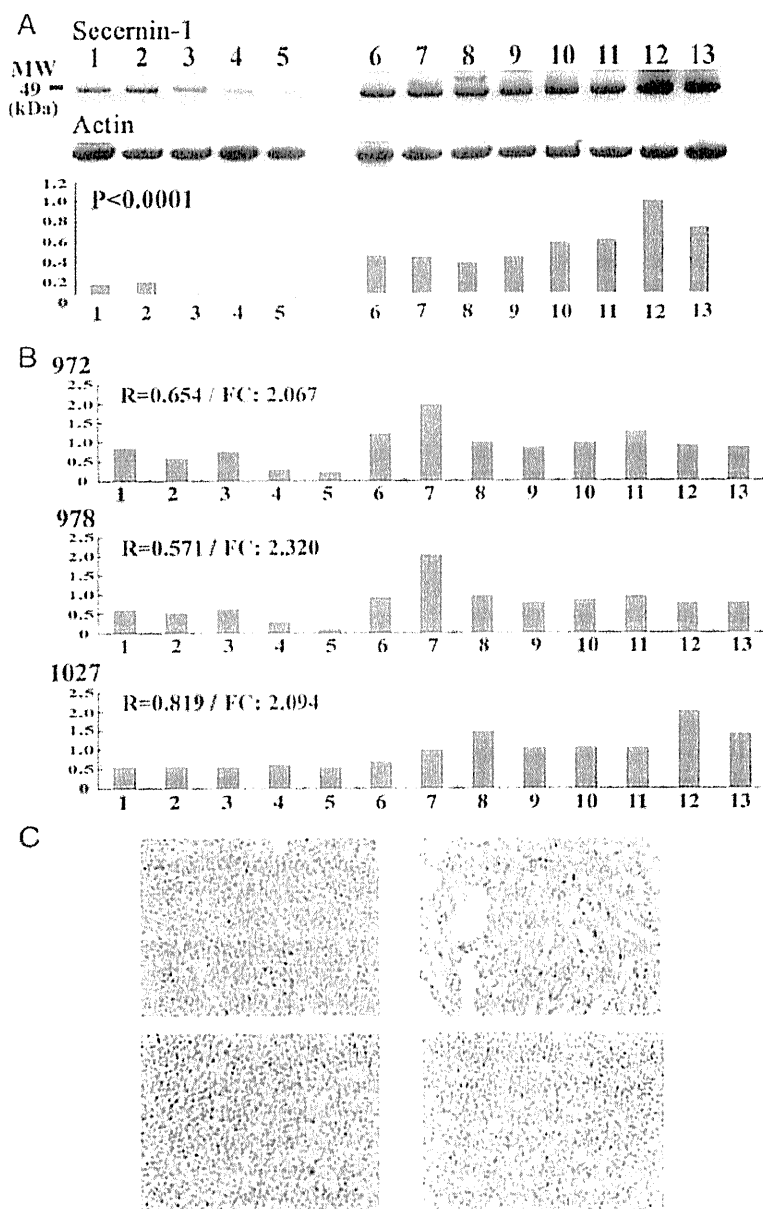


Fig. 2 – Validation of the differential expression of secernin-1 in the synovial sarcoma. (A) P-SS (cases 1 to 5) expressed secernin-1 at significantly lower levels than G-SS (cases 6 to 13). The case numbers correspond to those in Fig. 1. The Western blotting results and the bar plots demonstrate the secernin-1 expression levels (fold-change: 4.969, Mann-Whitney's test: $p < 0.0001$). (B) The bar plots demonstrate the expression levels of the three secernin-1 spots (No. 972, No. 978 and No. 1027) in the 13 synovial sarcoma samples examined (fold-change (FC): 2.067 for No. 972, 2.320 for No. 978 and 2.094 for No. 1027). The expression levels detected by 2D-DIGE correlated highly with the levels detected by the Western blotting analysis ($R = 0.654$ for No. 972, $R = 0.571$ for No. 978 and $R = 0.819$ for No. 1027). (C) Immunohistochemistry validates the correlation between secernin-1 expression and prognosis. Secernin-1 was overexpressed in the primary tumors of patients with a good prognosis (upper panel), while it was not expressed in the tumors of patients with a poor prognosis (lower panel). Note that secernin-1 was mainly expressed in the cytoplasm, consistent with a previous report [26], and a few cells showed the nuclear localization of secernin-1 (Supplemental Fig. 5).

Forty of the 45 patients had localized disease without distant metastases at the time of diagnosis. We performed a second univariate analysis for these 40 patients and found

that negative secernin-1 expression was a significant predictor of short tumor specific and metastasis free survival (Fig. 3C and D, $P = 0.0020$ and $P = 0.0016$, respectively, Supplemental

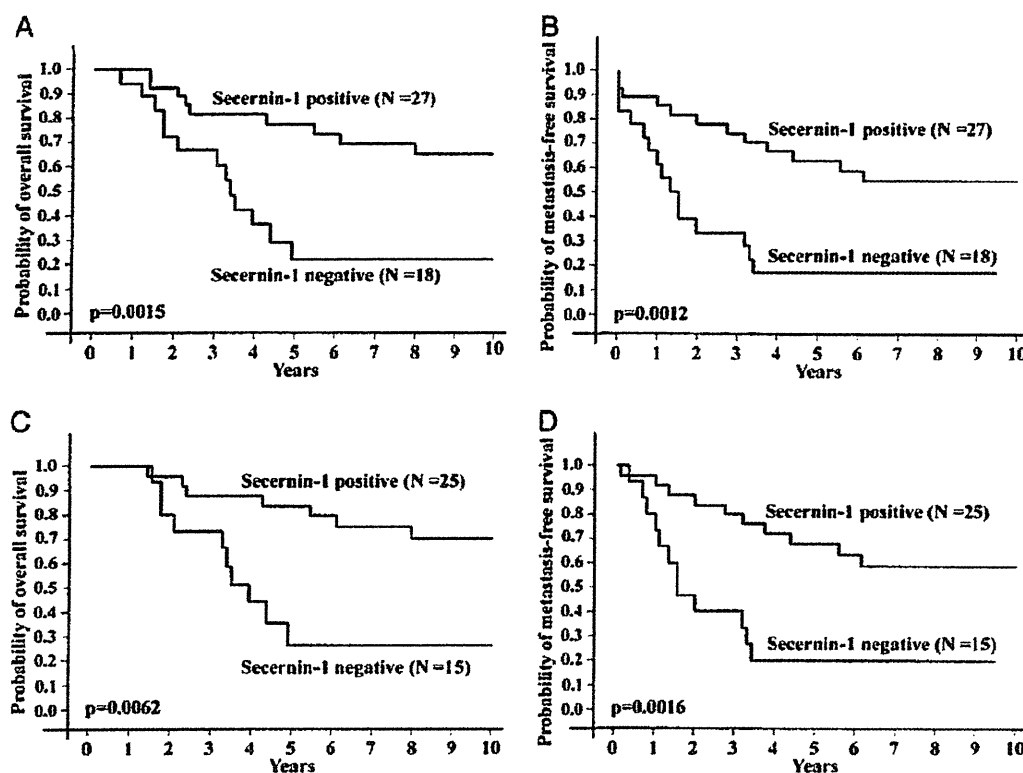


Fig. 3 – Prognostic value of secernin-1 expression examined immunohistochemically. (A) Secernin-1 expression in 45 primary tumor samples was predictive of the tumor specific survival period. **(B)** The metastasis free survival was significantly higher in the secernin-1 positive compared to the negative synovial sarcoma group. **(C and D)** The overall survival and metastasis free survival of the M0 synovial sarcoma patients correlated with secernin-1.

Table 5). A multivariate analysis also showed that negative secernin-1 expression was an independent prognostic factor for short tumor specific ($p=0.0480$) and metastasis free survival ($p<0.0001$) (Supplemental Table 5).

These data clearly indicate that prognosis relying solely on the established histological classification system is not sufficiently accurate to determine the post-operative therapeutic strategy for synovial sarcoma patients, and the use of secernin-1 expression may further refine the prognostic criteria so as to identify patients who may benefit from additional therapy.

4. Discussion

Immunohistochemical studies have previously resulted in the identification of candidate prognostic biomarkers in synovial sarcoma [10,14,32–42]. Although these studies furthered our understanding of the biology of synovial sarcoma, none of the reported candidate biomarkers was proven to be practical in a clinical setting to date. Apart from further validation studies on the aforementioned biomarkers, we need to discover novel prognostic biomarkers. The proteome is a functional translation of the genome, directly regulating cell phenotypes, and thus is a rich source of candidate biomarkers. For these

reasons, and to gain further molecular insight into the varying prognosis of patients with synovial sarcoma, we conducted the proteomics study on synovial sarcoma presented here, the first report employing a proteomic approach to examine prognostic biomarkers of synovial sarcoma.

With respect to 2D-DIGE technologies, especially fluorescent dyes, two types of fluorescent dyes are presently available for 2D-DIGE: CyDye DIGE Fluor minimal dye, and CyDye DIGE Fluor saturation dye [29]. The former labels a small portion of lysine residues; its sensitivity is similar to that of silver staining, and labeling with it does not change the electrophoretic mobility of the protein [29]. In contrast, the latter labels all reduced cysteine residues of the protein. As a result, the dye affects the electrophoretic mobility of the protein, thus resulting in a 100–200-fold higher sensitivity than CyDye DIGE Fluor minimal dye [29]. In this study, we used saturation labeling in order to provide higher quality data that would provide more information about the protein spots.

Several studies have demonstrated a lack of synovial differentiation in synovial sarcoma tumor cells, and have also shown that these tumors express markers of both epithelial and mesenchymal differentiations, although they do not resemble any specific tissue type, and their origin has been unknown [13,27,28]. Synovial sarcoma is now regarded as a neoplasm of “uncertain differentiation” [28]. Given their unclear backgrounds,

Table 3 - Uni- and multivariate analysis of prognostic factors and the relationship between clinico-pathological parameters and secemin-1 expression.

Variable	Number of cases	Tumor specific survival		Metastasis free survival		Multivariate analysis of tumor specific survival by Cox regression			Multivariate analysis of metastasis free survival by Cox regression			Secemin-1 negative (number of cases)	Secemin-1 positive (number of cases)	Correlation (secernin-1) χ^2 (p value)	
		5-years (%)	Log-rank (p value)	5-years (%)	Log-rank (p value)	P value	Relative risk	95% confidence interval	P value	Relative risk	95% confidence interval				
Age			0.3466		0.4239										0.7120
<35	26	52.6±9.7		38.5±9.6								11	15		
>35	19	63.2±11.1		51.5±11.8								7	12		
Gender			0.3087		0.1133										0.8050
F	26	59.4±10.0		53.3±9.9								10	16		
M	19	52.6±11.45		31.6±10.7								8	11		
Site			0.0796		0.2713										0.6710
Trunk	11	32.7±15.0		27.3±13.4								5	6		
Extremity	34	64.2±8.3		49.8±8.6								13	21		
Histology subtype			0.0136		<0.0001										0.7460
Monophasic	28	70.2±8.9		49.5±9.6								10	18		
Biphasic	13	46.2±13.8		46.2±13.8								6	7		
Poorly differentiated	4	0±0		0±0								2	2		
Fusion gene			0.1555		0.2005										0.1270
SYT/SSX1	23	69.3±9.7		56.2±10.4								6	17		
SYT/SSX2	8	45.0±18.8		25.0±15.3								5	3		
Not detected	14	-		-								7	7		
Size			0.2925		0.0384				0.0220	7.2	1.335-38.45				0.9000
<5 cm	18	64.2±11.8		58.8±11.9								7	10		
>5 cm	27	52.3±9.7		35.7±9.1								10	17		
Depth			0.5574		0.3179										0.3290
Superficial	3	66.7±27.2		66.7±27.2								2	1		
Deep	42	56.0±7.8		42.6±7.7								16	26		

MIB-1			0.0130	0.0049				0.0070	0.04	0.003-0.42								0.0530
<9%	4	100±0		75.0±21.9										1				3
10-29%	10	80.0±12.6		80.0±12.6										1				9
>30%	31	43.3±9.2		28.7±8.2										16				15
Grade			0.0003	<0.0001				0.0020	931.05	12.35-70130.10								0.0540
2	12	100±0		91.7±8.0										2				10
3	33	40.6±8.8		26.9±7.8										16				17
Stage			<0.0001	0.0703														0.7250
IIA	17	64.2±11.8		58.8±11.9										7				10
IIB	2	100±0		100±0										1				1
III	21	60.2±11.0		37.5±10.7										7				14
IV	5	0±0		-										3				2
Metastasis			<0.0001	-	<0.0001	48.40	6.0-387.8											0.3330
M0	40	63.9±7.8		-										15				25
M1	5	0±0		-										3				2
Local recurrence			0.2846	0.8770														0.1300
No recurrence	33	62.9±8.5		48.1±8.8										11				22
Recurrence	12	41.7±14.2		33.3±13.6										7				5
Adjuvant CTx			0.0827	0.1233														0.7140
Received	24	48.9±10.4		33.3±9.6										9				12
Not received	21	65.9±10.5		56.3±11.0										9				15
Adjuvant RTx			0.0537	0.0559														0.2240
received	9	88.9±10.5		66.7±15.7										2				7
Not received	36	48.2±8.6		38.9±8.1										16				20
Secernin-1			0.0015	0.0012	0.0190	4.70	1.3-17.3	0.0010	21.90	3.3-145.90								
Positive	27	77.6±8.1		62.8±9.4														
Negative	18	21.8±10.6		16.7±8.8														

HPF: high-power field.

it is impossible to compare normal tissues with tumor tissue in order to identify proteins corresponding to tumor-specific characteristics. In order to identify proteins corresponding to tumor progression and patient outcome, we defined the G-SS and P-SS groups using their different backgrounds and then compared the two groups. We identified twelve down-regulated and eight up-regulated proteins from synovial sarcoma cases with poor prognosis. Functional classification revealed that these identified proteins belonged to a variety of functional pathways. Synovial sarcoma is characterized by a translocation between the SYT gene and -SSX1, -SSX2 or -SSX4 [1–4]. Although the protein complexes involving the SYT/SSX fusion gene products have aberrant transcriptional activity and modulate the expression of a number of downstream target genes [43], the genes affected by the SYT/SSX fusion have not been reported yet. The altered transcriptional activity of the SYT/SSX protein may induce a large number of functional aberrations in synovial sarcoma, and the effects of SYT/SSX on gene expression may not be equal among the patients, resulting in the different prognosis observed.

Three variants of secernin-1 were highly expressed in the primary tumors of the patients with good prognosis. According to the DNA sequence, there are five alternative splicing variants for secernin-1 (GeneCards, <http://www.genecards.org>). The different variants may result in three protein spots for secernin-1 in our study. This is the first report of the prognostic value of secernin-1 expression, and the association of secernin-1 expression with synovial sarcoma has not been previously reported. Importantly, previous synovial sarcoma studies employing a global approach at the DNA and mRNA levels did not reveal any association of secernin-1 with synovial sarcoma [13–16]. These results suggest that the use of a proteomic approach can reveal unique molecular aspects of synovial sarcoma not visible through the use of other techniques (Supplemental Table 6).

Our results suggest that secernin-1 expression could be a novel prognostic biomarker for synovial sarcoma. As secernin-1 expression correlated with two important clinical endpoints, namely the metastatic potential and survival, it will give us the opportunity to establish improved prognostic modalities. Both uni- and multivariate analyses revealed that secernin-1 expression along with clinical stage (metastasis at diagnosis) was an independent prognostic factor for overall survival of patients with synovial sarcoma. With regard to the SYT-SSX1 fusions, there were no correlations between secernin-1 expression and the presence of fusion genes. Furthermore, secernin-1 expression was also a significant prognostic factor in patients with localized disease.

Secernin-1 is a cytosolic protein that stimulates exocytosis in mast cells [25,26]. However, the mechanisms underlying its involvement in exocytosis remain unresolved [25]. Secernin-1 might cause the recruitment of secretory granules to the site of exocytosis or increase granule swelling, core expulsion, or breakdown in tumor cells [25]. Cytosolic proteins that are capable of regulating exocytosis in permeabilized cell assays appear to fall into four major categories: 1) proteins that directly interact with the fusion machinery, 2) GTPases involved in intracellular signaling, 3) proteins involved in other intracellular signaling pathways, and 4) proteins involved in the regulation of PIP2 [26]. Notably, a number of GTP

binding proteins play a role in secretion. These molecules are also involved in numerous other physiological functions, so secernin-1 might also play different roles, other than exocytosis, in the cells [25].

Transferring the above to the clinic in the form of a practical application that would incorporate the examination of secernin-1 expression will be the next challenge. Secernin-1 was found to contain antigenic epitope peptides and could induce cytotoxic T cells which lysed the tumor cells expressing secernin-1, and was highly expressed in gastric cancer tissues compared with their normal counterparts [25]. Secernin-1 expression was exclusively observed in the testes and ovaries, being barely detected in the other normal organs [25]. The examination of secernin-1 expression has been applied in the development of cancer vaccines in gastric cancer [25]. The augmented expression of secernin-1 resulted in reduced colony formation [25]. Similar examinations in synovial sarcomas will pave a way to novel therapies, even if they have opposing expression patterns compared to gastric cancer [25]. Thus, when we consider its therapeutic application, knowledge of the functional contribution of secernin-1 to the malignant phenotypes is also important.

Examination of secernin-1 expression may allow the identification of the synovial sarcoma patients who are more likely to develop metastases after treatment. Similarly, the patients who have secernin-1 positive primary tumors may benefit by avoiding such intensified therapy.

5. Conclusion

In conclusion, we identified a possible correlation of 20 protein variants corresponding to 17 distinct gene products with parameters of clinical interest in synovial sarcoma. The secernin-1 has a potential to promote cancer progression and its expression was correlated with prognosis of synovial sarcoma in 45 cases. As the expression of secernin-1 could be monitored by immunohistochemistry, a routine examination in the hospitals, once the clinical utilities of secernin-1 was established, our findings will be applied to the clinical examination. Evaluation of secernin-1 expression may allow for the identification of the prognosis of synovial sarcoma patients who may benefit from more aggressive treatment.

Supplementary materials related to this article can be found online at doi:10.1016/j.jprot.2011.02.033.

Conflict of interest statement

The corresponding author had full access to all the data in the study and had final responsibility for the decision to submit the manuscript for publication. The corresponding author declares that there is no conflict of interest.

Acknowledgements

This work was supported by a grant from the Ministry of Health, Labor and Welfare, by the Program for Promotion of

Fundamental Studies in Health Sciences of the National Institute of Biomedical Innovation of Japan and by The Uehara Memorial Foundation. The excellent technical support of Kiyooki Nomoto, Chizu Kina, and Sachiko Miura in the immunohistochemical study, and Kano Nishiyama and Yukiko Fujie in electrophoresis is greatly appreciated.

REFERENCES

- [1] Trassard M, Le Doussal V, Hacene K, Terrier P, Ranchere D, Guillou L, et al. Prognostic factors in localized primary synovial sarcoma: a multicenter study of 128 adult patients. *J Clin Oncol* 2001;19(2):525–34.
- [2] Spillane AJ, A'Hern R, Judson IR, Fisher C, Thomas JM. Synovial sarcoma: a clinicopathologic, staging, and prognostic assessment. *J Clin Oncol* 2000;18(22):3794–803.
- [3] Lewis JJ, Antonescu CR, Leung DH, Blumberg D, Healey JH, Woodruff JM, et al. Synovial sarcoma: a multivariate analysis of prognostic factors in 112 patients with primary localized tumors of the extremity. *J Clin Oncol* 2000;18(10):2087–94.
- [4] Fletcher CDM UK, Mertens F. IARC Press: Lyon Pathol genetics tumours soft tissue bone 2002:200–4.
- [5] dos Santos NR, de Bruijn DR, van Kessel AG. Molecular mechanisms underlying human synovial sarcoma development. *Genes Chromosom Cancer* 2001;30(1):1–14.
- [6] Nagai M, Tanaka S, Tsuda M, Endo S, Kato H, Sonobe H, et al. Analysis of transforming activity of human synovial sarcoma-associated chimeric protein SYT-SSX1 bound to chromatin remodeling factor hBRM/hSNF2 alpha. *Proc Natl Acad Sci USA* 2001;98(7):3843–8.
- [7] Skytting B, Nilsson G, Brodin B, Xie Y, Lundeberg J, Uhlen M, et al. A novel fusion gene, SYT-SSX4, in synovial sarcoma. *J Natl Cancer Inst* 1999;91(11):974–5.
- [8] Clark J, Rocques PJ, Crew AJ, Gill S, Shipley J, Chan AM, et al. Identification of novel genes, SYT and SSX, involved in the t(X;18)(p11.2;q11.2) translocation found in human synovial sarcoma. *Nat Genet* 1994;7(4):502–8.
- [9] Ladanyi M, Antonescu CR, Leung DH, Woodruff JM, Kawai A, Healey JH, et al. Impact of SYT-SSX fusion type on the clinical behavior of synovial sarcoma: a multi-institutional retrospective study of 243 patients. *Cancer Res* 2002;62(1):135–40.
- [10] Antonescu CR, Kawai A, Leung DH, Lonardo F, Woodruff JM, Healey JH, et al. Strong association of SYT-SSX fusion type and morphologic epithelial differentiation in synovial sarcoma. *Diagn Mol Pathol* 2000;9(1):1–8.
- [11] Kawai A, Woodruff J, Healey JH, Brennan MF, Antonescu CR, Ladanyi M. SYT-SSX gene fusion as a determinant of morphology and prognosis in synovial sarcoma. *N Engl J Med* 1998;338(3):153–60.
- [12] Lee YF, John M, Falconer A, Edwards S, Clark J, Flohr P, et al. A gene expression signature associated with metastatic outcome in human leiomyosarcomas. *Cancer Res* 2004;64(20):7201–4.
- [13] Nagayama S, Katagiri T, Tsunoda T, Hosaka T, Nakashima Y, Araki N, et al. Genome-wide analysis of gene expression in synovial sarcomas using a cDNA microarray. *Cancer Res* 2002;62(20):5859–66.
- [14] Allander SV, Illei PB, Chen Y, Antonescu CR, Bittner M, Ladanyi M, et al. Expression profiling of synovial sarcoma by cDNA microarrays: association of ERBB2, IGFBP2, and ELF3 with epithelial differentiation. *Am J Pathol* 2002;161(5):1587–95.
- [15] Segal NH, Pavlidis P, Antonescu CR, Maki RG, Noble WS, DeSantis D, et al. Classification and subtype prediction of adult soft tissue sarcoma by functional genomics. *Am J Pathol* 2003;163(2):691–700.
- [16] Nielsen TO, West RB, Linn SC, Alter O, Knowling MA, O'Connell JX, et al. Molecular characterisation of soft tissue tumours: a gene expression study. *Lancet* 2002;359(9314):1301–7.
- [17] Petricoin EF, Ardekani AM, Hitt BA, Levine PJ, Fusaro VA, Steinberg SM, et al. Use of proteomic patterns in serum to identify ovarian cancer. *Lancet* 2002;359(9306):572–7.
- [18] Suehara Y, Kondo T, Fujii K, Hasegawa T, Kawai A, Seki K, et al. Proteomic signatures corresponding to histological classification and grading of soft-tissue sarcomas. *Proteomics* 2006;6(15):4402–9.
- [19] Kikuta K, Tochigi N, Shimoda T, Yabe H, Morioka H, Toyama Y, et al. Nucleophosmin as a candidate prognostic biomarker of Ewing's sarcoma revealed by proteomics. *Clin Cancer Res* 2009;15(8):2885–94.
- [20] Orimo T, Ojima H, Hiraoka N, Saito S, Kosuge T, Kakisaka T, et al. Proteomic profiling reveals the prognostic value of adenomatous polyposis coli-end-binding protein 1 in hepatocellular carcinoma. *Hepatology* 2008;48(6):1851–63.
- [21] Chen G, Gharib TG, Wang H, Huang CC, Kuick R, Thomas DG, et al. Protein profiles associated with survival in lung adenocarcinoma. *Proc Natl Acad Sci USA* 2003;100(23):13537–42.
- [22] Suehara Y, Kondo T, Seki K, Shibata T, Fujii K, Gotoh M, et al. Pftin as a prognostic biomarker of gastrointestinal stromal tumors revealed by proteomics. *Clin Cancer Res* 2008;14(6):1707–17.
- [23] Okano T, Kondo T, Fujii K, Nishimura T, Takano T, Ohe Y, et al. Proteomic signature corresponding to the response to gefitinib (Iressa, ZD1839), an epidermal growth factor receptor tyrosine kinase inhibitor in lung adenocarcinoma. *Clin Cancer Res* 2007;13(3):799–805.
- [24] Sabo E, Meitner PA, Tavares R, Corless CL, Lauwers GY, Moss SF, et al. Expression analysis of Barrett's esophagus-associated high-grade dysplasia in laser capture microdissected archival tissue. *Clin Cancer Res* 2008;14(20):6440–8.
- [25] Suda T, Tsunoda T, Uchida N, Watanabe T, Hasegawa S, Satoh S, et al. Identification of secernin 1 as a novel immunotherapy target for gastric cancer using the expression profiles of cDNA microarray. *Cancer Sci* 2006;97(5):411–9.
- [26] Way G, Morrice N, Smythe C, O'Sullivan AJ. Purification and identification of secernin, a novel cytosolic protein that regulates exocytosis in mast cells. *Mol Biol Cell* 2002;13(9):3344–54.
- [27] Haldar M, Hancock JD, Coffin CM, Lessnick SL, Capocchi MR. A conditional mouse model of synovial sarcoma: insights into a myogenic origin. *Cancer Cell* 2007;11(4):375–88.
- [28] Christopher D.M. Fletcher KKU, Fredrik Mertens. World health organization classification of tumours, pathology and genetics, tumours of soft tissue bone 2002.
- [29] Kondo T, Hirohashi S. Application of highly sensitive fluorescent dyes (CyDye DIGE Fluor saturation dyes) to laser microdissection and two-dimensional difference gel electrophoresis (2D-DIGE) for cancer proteomics. *Nat Protoc* 2006;1(6):2940–56.
- [30] Kondo T, Hirohashi S. Application of 2D-DIGE in cancer proteomics toward personalized medicine. *Meth Mol Biol* 2009;577:135–54.
- [31] Takenaka S, Ueda T, Naka N, Araki N, Hashimoto N, Myoui A, et al. Prognostic implication of SYT-SSX fusion type in synovial sarcoma: a multi-institutional retrospective analysis in Japan. *Oncol Rep* 2008;19(2):467–76.
- [32] Antonescu CR, Leung DH, Dudas M, Ladanyi M, Brennan M, Woodruff JM, et al. Alterations of cell cycle regulators in localized synovial sarcoma: a multifactorial study with prognostic implications. *Am J Pathol* 2000;156(3):977–83.
- [33] Kawauchi S, Fukuda T, Oda Y, Saito T, Oga A, Takeshita M, et al. Prognostic significance of apoptosis in synovial

- sarcoma: correlation with clinicopathologic parameters, cell proliferative activity, and expression of apoptosis-related proteins. *Mod Pathol* 2000;13(7):755–65.
- [34] Kawauchi S, Goto Y, Liu XP, Furuya T, Oga A, Oda Y, et al. Low expression of p27(Kip1), a cyclin-dependent kinase inhibitor, is a marker of poor prognosis in synovial sarcoma. *Cancer* 2001;91(5):1005–12.
- [35] Hasegawa T, Yokoyama R, Matsuno Y, Shimoda T, Hirohashi S. Prognostic significance of histologic grade and nuclear expression of beta-catenin in synovial sarcoma. *Hum Pathol* 2001;32(3):257–63.
- [36] Saito T, Oda Y, Sakamoto A, Tamiya S, Kinukawa N, Hayashi K, et al. Prognostic value of the preserved expression of the E-cadherin and catenin families of adhesion molecules and of beta-catenin mutations in synovial sarcoma. *J Pathol* 2000;192(3):342–50.
- [37] Izumi T, Oda Y, Hasegawa T, Nakanishi Y, Kawai A, Sonobe H, et al. Dysadherin expression as a significant prognostic factor and as a determinant of histologic features in synovial sarcoma: special reference to its inverse relationship with E-cadherin expression. *Am J Surg Pathol* 2007;31(1):85–94.
- [38] Oda Y, Ohishi Y, Saito T, Hinoshita E, Uchiumi T, Kinukawa N, et al. Nuclear expression of Y-box-binding protein-1 correlates with P-glycoprotein and topoisomerase II alpha expression, and with poor prognosis in synovial sarcoma. *J Pathol* 2003;199(2):251–8.
- [39] Oda Y, Sakamoto A, Saito T, Kinukawa N, Iwamoto Y, Tsuneyoshi M. Expression of hepatocyte growth factor (HGF)/scatter factor and its receptor c-MET correlates with poor prognosis in synovial sarcoma. *Hum Pathol* 2000;31(2):185–92.
- [40] Ito T, Ouchida M, Morimoto Y, Yoshida A, Jitsumori Y, Ozaki T, et al. Significant growth suppression of synovial sarcomas by the histone deacetylase inhibitor FK228 in vitro and in vivo. *Cancer Lett* 2005;224(2):311–9.
- [41] Ishibe T, Nakayama T, Okamoto T, Aoyama T, Nishijo K, Shibata KR, et al. Disruption of fibroblast growth factor signal pathway inhibits the growth of synovial sarcomas: potential application of signal inhibitors to molecular target therapy. *Clin Cancer Res* 2005;11(7):2702–12.
- [42] Nakagawa Y, Numoto K, Yoshida A, Kunisada T, Ohata H, Takeda K, et al. Chromosomal and genetic imbalances in synovial sarcoma detected by conventional and microarray comparative genomic hybridization. *J Cancer Res Clin Oncol* 2006;132(7):444–50.
- [43] Xie Y, Tornkvist M, Aalto Y, Nilsson G, Gimita L, Nagy B, et al. Gene expression profile by blocking the SYT-SSX fusion gene in synovial sarcoma cells. Identification of XRCC4 as a putative SYT-SSX target gene. *Oncogene* 2003;22(48):7628–31.

Use of Vascularized Free Fibular Head Grafts for Upper Limb Oncologic Reconstruction

Satoshi Onoda, M.D.
Minoru Sakuraba, M.D.
Takayuki Asano, M.D.
Shimpei Miyamoto, M.D.
Yasuo Beppu, M.D.
Hirokazu Chuman, M.D.
Akira Kawai, M.D.
Fumihiko Nakatani, M.D.
Yoshihiro Kimata, M.D.

Chiba, Tokyo, and Okayama, Japan

Background: Transfer of a vascularized fibular graft is the method of first choice for reconstruction of defects of long bones. In particular, the vascularized fibula head graft is preferred for patients with bone defects of the upper limb involving the distal radius or the proximal humerus. The aim of the present study was to analyze the operative results, complications, and postoperative function after vascularized fibula head graft transfer and the indications for this procedure.

Methods: From 1998 through 2008, vascularized fibula head graft transfer was performed in eight patients to reconstruct bone defects following resection of tumors of the upper limb. The primary site of the tumor was the proximal humerus in four patients and the distal radius in four patients. The postoperative course of the transferred bone was examined, and functional results were evaluated.

Results: All vascularized fibula head grafts were transferred successfully. During the follow-up period, absorption of the transferred fibula head was not observed. The mean overall functional rating of the reconstructed shoulder joint was 70 percent. The range of motion of the reconstructed wrist joint showed no specific patterns, and instability of the wrist joint was observed in only one case.

Conclusions: The authors believe that the vascularized fibula head graft transfer is a safe and reliable method for reconstructing the upper limb, especially for patients with a defect of the distal radius or the proximal humerus. This procedure is also useful for pediatric patients, in whom bone growth is expected after transplantation, and for salvage procedures after reconstructive materials of an artificial joint have failed. (*Plast. Reconstr. Surg.* 127: 1244, 2011.)

Transfer of a vascularized fibular graft is the method of first choice for the reconstruction of defects of long bones. In particular, the vascularized fibula head graft is preferred for reconstruction of bone defects of the upper limbs involving the distal end of the radius. After transfer of a vascularized fibula head graft for reconstruction of the distal radius was first described in 1979 by Pho, the vascularized fibula head graft became the first choice for reconstruction of such defects at many institutions.¹⁻³ At our institution, the vascularized fibula head graft has been used to reconstruct the proximal humerus and the distal radius. The aim of the present study was to analyze

the operative results, complications, and postoperative function after vascularized fibula head graft transfer and the indications for this procedure.

PATIENTS AND METHODS

From 1998 through 2008, vascularized fibula head grafts were transferred at the National Cancer Center Hospital to reconstruct the upper limb following resection of tumors of the proximal humerus in four patients and the distal end of radius in four patients. The eight patients (four men and four women) ranged in age from 4 to 57 years (mean, 32 years). Seven patients had a primary malignant tumor of the upper limb, and one patient had failure of a prosthetic of the proximal humerus. The initial pathologic diagnoses were as follows: giant cell tumor in four patients, chondrosarcoma in three patients, and synovial sarcoma in one patient.

From the Division of Plastic Surgery, National Cancer Center Hospital Central and East; the Division of Orthopedic Surgery, National Cancer Center Hospital; and the Department of Plastic and Reconstructive Surgery, Graduate School of Medicine, Dentistry, and Pharmaceutical Science, University of Okayama.

Received for publication May 23, 2010; accepted September 21, 2010.

Copyright ©2011 by the American Society of Plastic Surgeons

DOI: 10.1097/PRS.0b013e318205f34b

Disclosure: *The authors have no financial interest to declare in relation to the content of this article.*

Marginal resection was performed in four patients with giant cell tumors. Wide resection with a surgical margin of 2 cm was performed in three patients with chondrosarcoma. Patient 6, who had a synovial sarcoma, was treated with multimodal therapy, including preoperative chemotherapy, surgery, and postoperative radiation therapy. Wide resection of the synovial sarcoma was performed with an adequate surgical margin. In all patients, the articular surface of the head of the radius or humerus was involved by tumor and resected. The mean length of bone defects was 11.8 cm (range, 5 to 23 cm) (Table 1).

Bony defects were reconstructed with a vascularized fibula head graft including the biceps femoris tendon, which was attached to the fibular head in all patients. The biceps tendon was used to suspend the head of the fibula from the acromion of the scapula in patients 1, 2, and 4. In patient 3, arthrodesis of the shoulder joint was performed between the scapula and the transferred bone with a fixating screw and the biceps tendon. For defects of the distal radius, arthroplasty was performed with the biceps tendon between the head of the fibula and the carpal bones (Table 1).

The vascular pedicle of the graft comprised peroneal vessels in three patients, anterior tibial vessels in four patients, and lateral inferior genicular vessels in one patient. The recipient vessels were branches of the deep brachial artery and deep brachial vein in one patient, the posterior circumflex humeral artery and vein in one patient, the subscapular artery and vein in one patient, the thoracodorsal artery and vein in one patient, and the radial arteries and veins and cephalic veins in four patients. In two patients, reverse arterial anastomoses were needed between the distal portion of the anterior tibial artery and the radial artery or the thoracodorsal artery. Vein grafts were needed at the arterial anastomoses in three patients. In patient 2, flow-through type microvascular anastomoses were performed between the circumflex scapular artery and the anterior tibial artery. For all cases, we did not perform the special fixation between the residual fibula and the ankle joint after flap harvesting.

The postoperative course of the transferred bone was examined with radiography, and the degree of bone union, absorption, fracture, and donor site (Fig. 1) were evaluated. Functional results were evaluated with the rating system of the Musculoskeletal Tumor Society in four patients who underwent reconstruction of the proximal humerus (Table 2).⁴ The range of motion and stability of the wrist joint

Table 1. Details of the Eight Patients in Whom Vascularized Fibula Head Grafts Were Transferred to the Upper Limbs

Patient	Age (yr)	Sex	Diagnosis	Part of Defect	Graft Length (cm)	Vascular Pedicle	Shoulder or Wrist Joint	Vein Graft	Anastomosis Style Artery/Vein	Radiation Therapy	Other Factors
1	4	M	Chondrosarcoma	PH	14	PAV	Plasty	None	A/A	None	Child case
2	32	F	Chondrosarcoma	PH	13	ATAV	Plasty	Artery, 3 cm	A/A	None	
3	51	M	Chondrosarcoma	PH	23	PAV	Fixation	None	A/A	None	
4	40	F	GCT	PH	11	ATAV	Plasty	None	R/A	None	Prosthetic failure
5	28	M	GCT	DR	7	ATAV	Plasty	Artery, 3 cm	A/A	None	
6	57	F	Synovial sarcoma	DR	13	PAV	Plasty	None	R/A	36 Gy (postoperative)	
7	23	F	GCT	DR	5	ILGAV	Plasty	Artery, 3 cm	A/A	None	Recurrent disease
8	21	M	GCT	DR	8	ATAV	Plasty	None	A/A	None	

GCT, giant cell tumor; PH, proximal humerus; DR, distal radius; PAV, peroneal artery and vein; ATAV, anterior tibial artery and vein; ILGAV, inferior lateral genicular artery and vein; A, anterograde style; R, retrograde style; M, male; F, female.

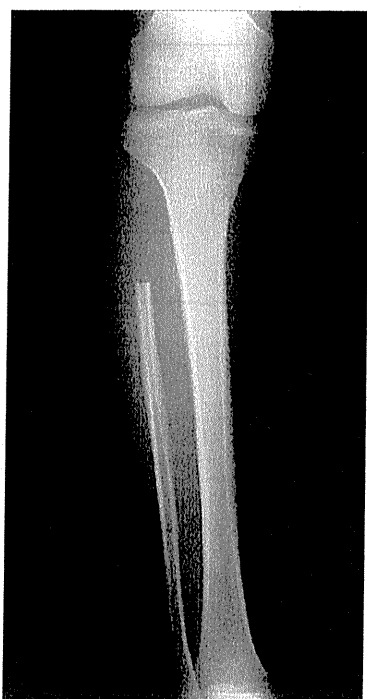


Fig. 1. Radiograph of patient 5 obtained 1 year after the fibula head had been harvested.

were evaluated in four patients who underwent reconstruction of the distal radius.

RESULTS

All vascularized fibula head grafts were transferred successfully. However, surgical débridement was required for necrosis of a parascapular flap that was transferred simultaneously with the vascularized fibula head graft in patient 4. Bone union between the transferred fibula bone and

residual bone was achieved within 6 months in all except two patients (patients 2 and 4). Although pseudoarthrosis was observed in these two patients (25 percent), additional surgery was not performed because clinical symptoms were absent and because the patients refused further surgery. Furthermore, the bone-fixing plates became deviated in patient 3 (12.5 percent), and secondary fixation was required 2 months after surgery.

Donor-site morbidity was observed in one patient: peroneal nerve paralysis (12.5 percent) occurred but resolved spontaneously with conservative treatment within 3 months. Regarding the flap donor site, there were no cases that showed instability of an ankle or the knee joint or gait disturbance during the follow-up period. The mean follow-up period was 4 years 6 months (range, 9 months to 10 years). During the follow-up period, absorption of the transferred fibula head was not observed in any of the patients (Table 3).

The overall functional rating of the Musculoskeletal Tumor Society scores after reconstruction of the proximal humerus were 73, 63, 80, and 63 percent in patients 1 through 4, respectively; and the mean functional rating of the reconstructed shoulder joint was 70 percent (Table 4). According to the Musculoskeletal Tumor Society scores, a score of 1 is the worst and a score of 5 is the best for each item. The results with regard to pain and manual dexterity were satisfactory, with scores in all patients of 5. However, the function and positioning of the hand were unsatisfactory; in one patient it was 3, and the other three patients had a score of 1 or 2 for each item. The Musculoskeletal Tumor Society scores were similar in all patients who had undergone reconstruction of the proximal humerus.

Table 2. Functional Rating System of the Musculoskeletal Tumor Society for the Upper Extremity

	Rating					
	5	4	3	2	1	0
Pain	None	Intermediate	Modest/ nondisabling	Intermediate	Moderate/ intermittently disabling	Severe/ continuously disabling
Function	No restrictions	Intermediate	Recreational restrictions	Intermediate	Partial occupational restriction	Total occupational restriction
Emotional acceptance	Enthusiastic	Intermediate	Satisfied	Intermediate	Accepts	Dislikes
Positioning of the hand	Unlimited	Intermediate	Not above shoulder or no pronation or supination	Intermediate	Not above waist	None
Manual dexterity	No limitation	Intermediate	Loss of movement	Intermediate	Cannot pinch	Cannot grasp
Lifting ability	Normal load	Intermediate	Limited	Intermediate	Helping only	Cannot help

Table 3. Postoperative Course of the Eight Patients

Patient	Postoperative Ossification (mo)	Response	Current Condition	Absorption	Follow-Up Period	Prognosis
1	1	Follow-up	Good	None	1 yr 8 mo	CDF
2	None	Follow-up	False joint	None	6 yr 9 mo	DOD
3	2	Refixation	Good	None	6 yr 6 mo	CDF
4	None	Follow-up	False joint	None	10 yr	CDF
5	3	Follow-up	Good	None	9 yr 6 mo	CDF
6	4	Reoperation (débridement)	Good	None	2 yr 3 mo	CDF
7	6	Follow-up	Good	None	4 yr 5 mo	CDF
8	3	Follow-up	Good	None	9 mo	CDF

CDF, continuously disease-free; DOD, died of disease.

Table 4. Musculoskeletal Tumor Society Scores

Patient	Pain	Function	Emotional Acceptance	Positioning of Hand	Manual Dexterity	Lifting Ability	Overall Functional Rating (%)
1	5	2	5	2	5	3	73
2	5	1	3	2	5	3	63
3	5	3	5	3	5	3	80
4	5	1	3	2	5	3	63
Mean	5	1.75	4	2.25	5	3	70

The range of motion and stability of the wrist joint were examined in patients who had undergone reconstruction of the distal radius (Table 5). No specific patterns of range of motion were found. Because of instability of the wrist, patient 6 used wrist joint orthotics. Wrist joint instability was absent in the other patients.

DISCUSSION

Procedures for functional reconstruction of bone defects of the upper limb include clavicle pro humero⁵ and the use of artificial joint materials, free bone grafts, vascularized bone grafts, and bone cement. Of these procedures, transfer of a vascularized fibula graft is the most widely used. In particular, the fibula bone graft containing the fibula head is suitable for reconstructing bone defects, including the shoulder or wrist joint, because of the anatomical similarity of the surfaces of these joints to the fibular head. Experimental applications of this procedure have been well described.⁶⁻⁹ The advantages of the vascularized fibula head graft are prevention of surgical infection and bone absorption, because of its sufficient blood flow, and good bone union between the

residual bone and transferred bone. Furthermore, the biceps femoris tendon attached to the fibula head facilitates arthroplasty.

Vascular Anatomy of the Vascularized Fibula Head Graft

When a vascularized fibula head graft is transferred, the anatomical territory of the vascular pedicle should be considered. Taylor et al. have reported a reliable blood supply from the anterior tibial artery to the proximal epiphysis and the proximal two-thirds of the diaphysis of the fibula.¹⁰ Mozaffarian et al. performed an anatomical study of the fibula head using fresh cadavers. According to that study, the anastomotic system between the anterior tibial artery and the peroneal artery are efficient enough to permit transfer of proximal fibular epiphysis and its adjacent 13 cm of diaphysis.¹¹ Innocenti et al. reported that the recurrent epiphyseal branch arises from the anterior tibial artery approximately 2 cm from its origin¹² (Fig. 2). In contrast, the dominant blood supply to the distal two-thirds of the fibula comes from the peroneal artery and vein. Therefore, when a short vascularized fibula head graft is to be transferred,

Table 5. Range of Motion and Grip Strength

Patient	Flexion (degrees)	Extension (degrees)	Pronation (degrees)	Supination (degrees)	Instability
5	70	20	90	40	None
6	10	20	20	20	None
7	20	30	30	30	Present
8	50	50	80	0	None

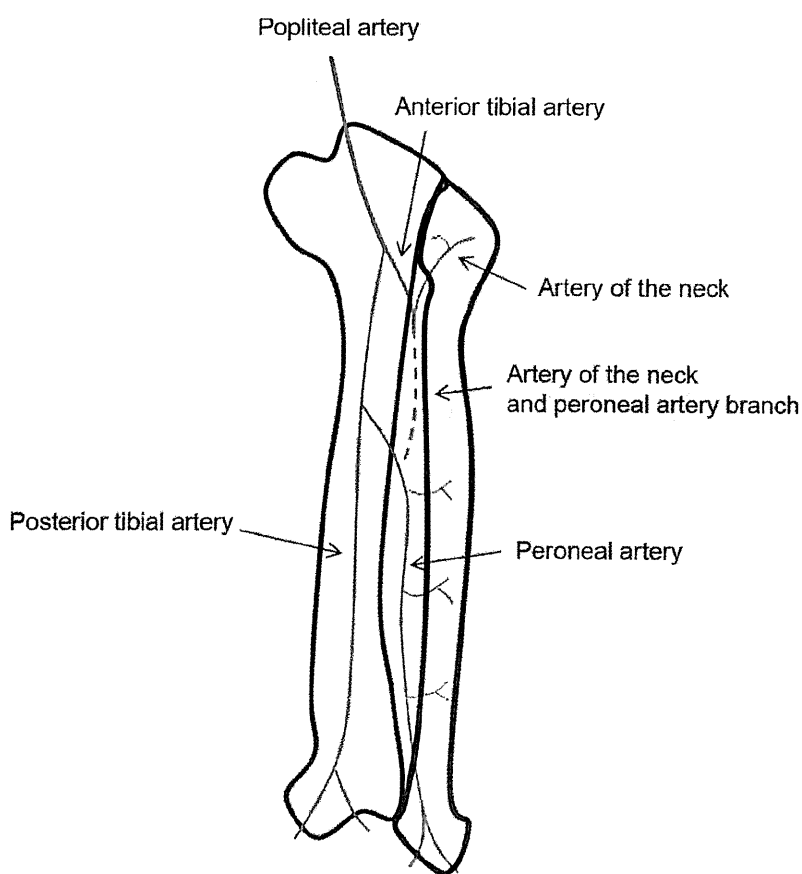


Fig. 2. Vascular anatomy of the fibula head.

we use the anterior tibial vessels as the vascular pedicle. In patients who require a long vascularized fibula head graft, we usually choose the peroneal vessels as the vascular pedicle. In the present study, the anterior tibial vessels were used as the vascular pedicle in four patients. In other cases, the peroneal vessels or inferior genicular vessels were used. In patients with giant cell tumors of the distal radius, bony defects were comparatively short, and the pedicle usually consisted of anterior tibial vessels. The blood flow to both the fibula head and the peripheral part of the fibula should be considered in patients with long bone defects. If anterior tibial vessels are used as the vascular pedicle in patients with long bone defects, the blood flow to the distal side of the graft may be poor, and bone union between the transferred bone and residual bone might not be obtained. In this series, pseudoarthroses were formed without sufficient bone union in two patients in whom anterior tibial vessels had been used as vascular pedicles. In contrast, when peroneal vessels were used as the vascular pedicle for a long vascularized

fibula head graft, the blood flow to the distal end was good, but the blood flow to the fibula head was poor. However, in patient 3, in whom peroneal vessels were used as the vascular pedicle, hemorrhage from the fibular head was observed after microvascular anastomosis. Furthermore, absorption of the head fibula was not observed during postoperative follow-up.

In patients 2 and 4, in whom short bony defects of the proximal humerus were reconstructed, anterior tibial vessels were used as the vascular pedicle. In both of these patients, bone fractures occurred between the transferred fibula and the residual bone, and pseudoarthroses were formed. The fractures were thought to have been caused by external force, defects of plating fixation and, most importantly, inadequate blood flow to the peripheral part of the transferred fibula. Ad-El et al. have reported that a sufficient blood supply was obtained both in the diaphysis of a long fibular graft and in the fibular head by using both the peroneal artery and the specific branch to the fibular head as a bipediced free flap.¹³ However,

in clinical practice, such problems as securing recipient vessels and using a cumbersome operating procedure may be encountered during reconstruction with bipediced flaps.

In patients 1, 3, and 6, peroneal vessels were used as vascular pedicles. For patient 1, an infant, two-thirds of the total length of the fibula (14 of 21 cm) was used (Figs. 3 and 4). In the three

patients in whom peroneal vessels were used, good blood flow to the fibular head was recognized intraoperatively. In all of these patients, the fibula head was not absorbed, and good bone union was obtained between the transferred fibula and the residual bone. For this reason, using peroneal vessels as vascular pedicles for the fibula head is appropriate for reconstructing long bone defects.

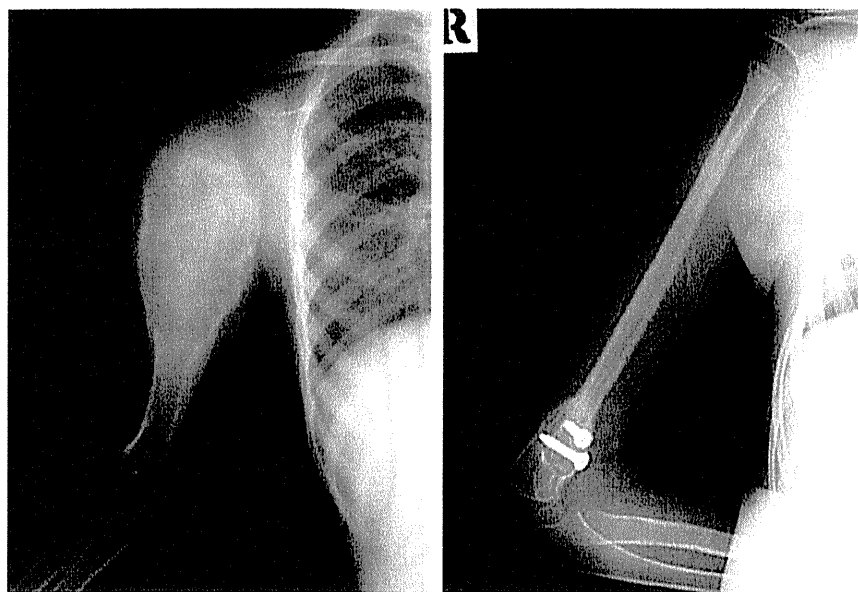


Fig. 3. Patient 1, a 4-year-old boy, presented with chondrosarcoma of the proximal humerus. (Left) Preoperative radiograph showed a $10 \times 14 \times 7$ -cm tumor. (Right) Radiograph obtained 3 months postoperatively showed good ossification between the transferred and residual bone.



Fig. 4. (Left) At 3 months postoperatively, the patient could grip a book with the affected limb. (Right) At 3 months postoperatively, the patient demonstrates elevation of the upper limb.

Our policy for choosing the vascular pedicle for vascularized fibula head grafts is as follows. For patients in the growing years, the first choice is anterior tibial vessels, because of the blood flow to the epiphyseal line. When the bone defect extends farther than the proximal two-thirds of the diaphysis of the fibula, we choose bipediced reconstruction or peroneal vessels after having confirmed the bleeding from the fibula head. For adults with bone defects shorter than 10 cm, anterior tibial vessels are recommended as the vascular pedicle of the vascularized fibula head graft. When bone defects in adults are longer than 10 cm, peroneal vessels should be used, because the blood supply to both the head and peripheral part of fibula is more secure (Fig. 5).

When anterior tibial vessels are used, the vascular pedicle of the vascularized fibula head graft may be too short. In such cases, a vein graft interposition is required between the flap and the recipient vessel. In our series, a vein graft was used for the arterial anastomosis in three cases, including two cases in which the anterior tibial artery was used as the flap pedicle and one case in which the inferior lateral genicular artery was used. Another procedure to compensate for a short vascular pedicle is to use the anterior tibial artery in a reverse manner. Sawaizumi et al. have described a free vascularized epiphyseal transfer design based on reversed anterior tibial vessels. The length of the vascular pedicle is approximately 8 cm.¹⁴ We used this procedure in patients 4 and 6. In contrast, a vein graft was not needed for venous anastomosis. Fur-

thermore, our vascularized fibula head grafts based on peroneal vessels had long pedicles, and additional vein grafts were not needed.

Postoperative Function

Shoulder Joint

The mean overall functional score in patients who underwent reconstruction of the proximal humerus was 70 percent (range, 63 to 80 percent). The elevation of the shoulder was a minor possibility, and physical limitation of the elbow joint and the wrist joint was not found in any of our patients. In each subject, scores were higher with regard to pain and manual dexterity and were lower with regard to function and positioning of the hand. Our results after reconstruction of the proximal humerus were similar to those of O'Connor et al.¹⁵ These unsatisfactory functional results can be attributed to the extended dissection of the periarticular tissue, muscles, and nerves of the shoulder. Although the stumps of the deltoid muscle and rotator cuff were sutured with transferred bone to increase postoperative function, the functional result was still unsatisfactory.¹⁶ The highest Musculoskeletal Tumor Society score (80 percent) was in a patient who had undergone shoulder joint fixation. In this case, plate fixation from a shoulder joint to a residual bone of the elbow joint neighborhood was performed. Certain solidity of the transferred bone and the residual bone was achieved, and it was thought that good

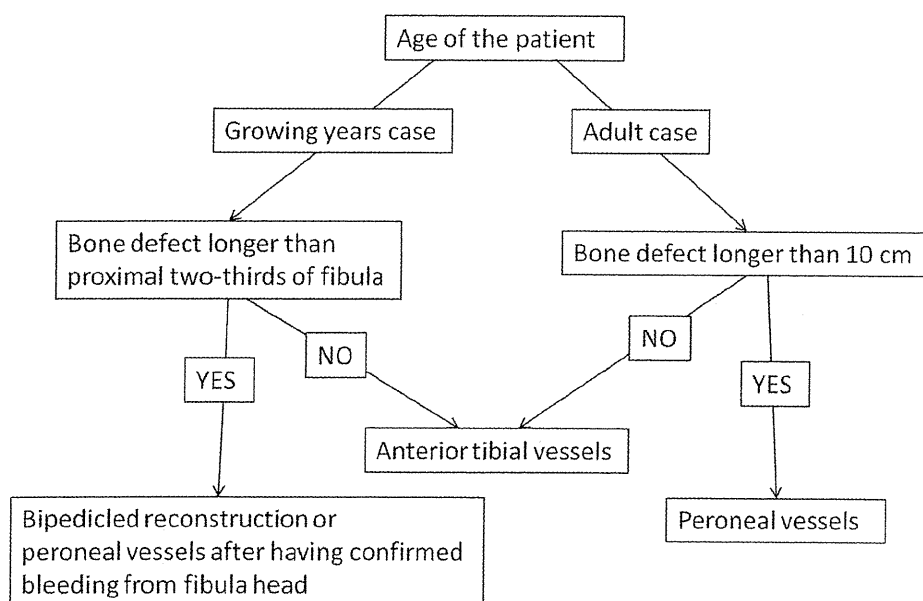


Fig. 5. Algorithm for selecting vascular pedicles of the fibula head graft.

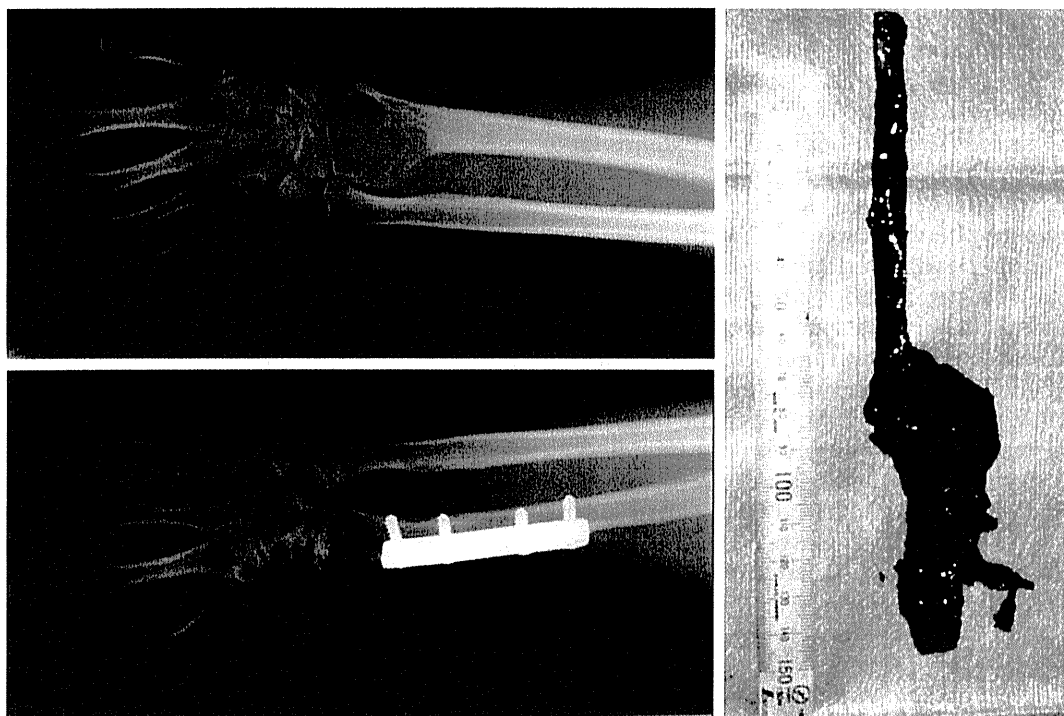


Fig. 6. Patient 5, a 28-year-old man, presented with a giant cell tumor of the distal radius. (*Above, left*) Preoperative radiograph shows a $48 \times 38 \times 35$ -mm tumor. (*Right*) Harvested 7-cm-long vascularized fibula head graft. (*Below, left*) Radiograph obtained 3 years postoperatively shows good ossification between the transferred bone and the residual bone.

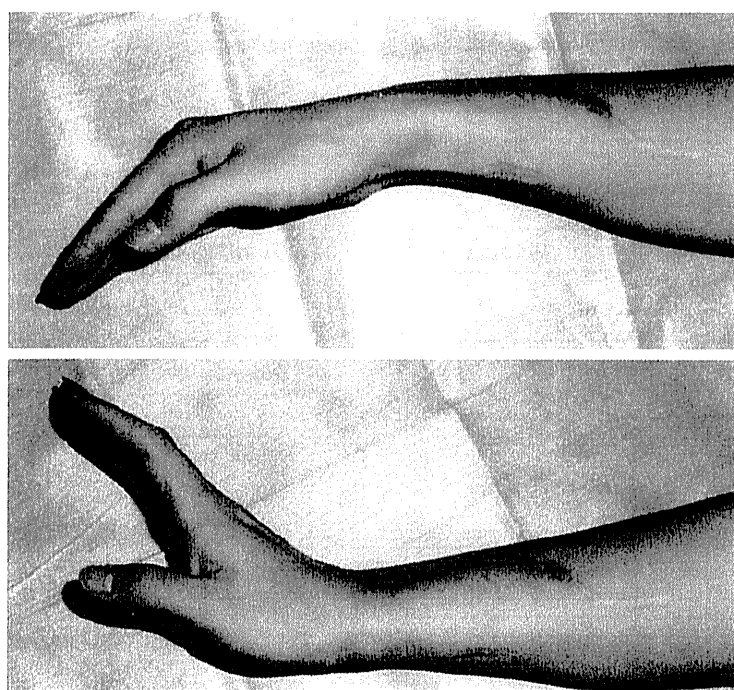


Fig. 7. At 3 years postoperatively, the patient demonstrates (*above*) extension and (*below*) flexion of the wrist joint.

postoperative function was obtained. Fuchs et al. reported that good shoulder function was obtained by shoulder arthrodesis.¹⁷ Like this case, the arthrodesis plate fixation should be considered in the comparatively long bone defect case in an adult patient. The vascularized fibula head graft has a rich blood flow and can be used safely for reconstruction of long bone defects, in comparison with osteoarticular allograft.¹⁸ Nishida et al. reported the ratio of complications with reconstruction after resection of the proximal humerus.¹⁹ Our results after reconstruction of the proximal humerus were comparatively better than other reports.

Tumors of the proximal humerus appear more commonly during infancy and adolescence. The difference in arm length attributable to subsequent growth becomes a major problem for these patients. With the vascularized fibula head graft, postoperative bone growth can be expected by transferring the epiphyses at the same time, and this is the major characteristic of this procedure. For this reason, the growing child is the ideal patient for vascularized fibula head graft transfer.²⁰

Distal Radius

The function of the wrist joint after reconstruction of the distal radius showed no specific patterns. The range of motion of the wrist differed greatly between patients 5 and 7 despite the similar primary diseases and ages of the patients (Figs. 6 and 7). This difference in range of motion was attributable to scar tissue from an operation performed 5 years earlier. In patient 6, the range of motion of the wrist joint was worse than in other patients, and additional surgery was needed to treat exposure of the transferred bone and infection 2 years after vascularized fibula head graft transfer. In this patient, wide resection of the surrounding soft tissue and postoperative irradiation were required for treatment of the tumor. Multimodal therapy or repeated surgery can impair the postoperative function of the wrist joint. In contrast, the range of motion in patients with giant cell tumors was good. Giant cell tumors have a predilection for the distal radius but are benign and seldom require wide resection involving the surrounding soft tissue.^{21–23} For this reason, satisfactory postoperative range of motion is more easily obtained in cases of giant cell tumor than in patients with malignant tumors. Giant cell tumor is the best indication for wrist joint reconstruction with a vascularized fibula head graft.

We performed wrist arthroplasty with the sling method in all cases. The transferred vascularized fibula head graft was slung over the carpal bones using the laden biceps femoris tendon on the fib-

ula head. Minami et al. have reported that a partial wrist arthrodesis with a vascularized fibular shaft graft is a more useful and reliable procedure for treating giant cell tumors of the distal radius than wrist arthroplasty with a vascularized fibular head graft.²⁴ However, the wrist joint becomes completely immobile when it is fixed rigidly by means of arthrodesis. Therefore, the sling method is our first choice for wrist joint reconstruction with a vascularized fibula head graft, because the mobility of the wrist joint is preserved. However, arthrodesis is indicated in cases similar to patient 6, in whom wide resection of the periarticular tissue was performed. The most important point regarding reconstruction of the wrist joint is that the most suitable procedure should be chosen for individual patients, with consideration of the primary disease, the extent of dissection, age, and other factors.

CONCLUSIONS

Transfer of a vascularized fibula head graft is a delicate, high-risk operation even if performed by experienced orthopedic or plastic surgeons.²⁵ The procedure for reconstruction of the upper limbs must be decided on the basis of the length of the bone defect, the extent of dissection, preoperative or postoperative adjuvant therapy, the frequency of complications, patient age, and patient preference. The upper limbs are common sites of giant cell tumors and chondrosarcomas. These tumors have a good prognosis, and transfer of a vascularized fibula head graft for reconstruction of defects of the upper limbs must be performed in these patients to regain function postoperatively. Patients with benign tumors are good candidates for vascularized fibula head graft transfer. However, for patients with malignant tumors who have undergone wide resection, the reconstruction method, including the arthrodesis, must be considered on an individual basis. Transfer of a vascularized fibula head graft is appropriate for reconstruction in infants, in whom subsequent bone growth is expected, and for salvage procedures after failure of artificial materials.

Satoshi Onoda, M.D.

Plastic and Reconstructive Surgery
Okayama University Graduate School of Medicine
2-5-1, Shikata-cho
Okayama 700-8558, Japan

PATIENT CONSENT

Parents or guardians provided written consent for the use of the patient's images.